Refereed Proceedings

The 13th International Conference on Fluidization - New Paradigm in Fluidization Engineering

Engineering Conferences International *Year* 2010

NUMERICAL EXPERIMENT ON EFFECT OF SURFACE ROUGHNESS FOR HEAT AND FLOW AROUND TWO CONTACTING PARTICLES

Azri bin Alias*

Kuwagi K., Bin Mokhtar M.A. Takami T.†

Horio M.‡

*Okayama University of Science, takumi_fujiwara84@yahoo.com

†Okayama University of Science

‡Tokyo University of Agriculture and Technology

NUMERICAL EXPERIMENT ON EFFECT OF SURFACE ROUGHNESS FOR HEAT AND FLOW AROUND TWO CONTACTING PARTICLES

Azri bin Alias[a], Kuwagi K.[a], Bin Mokhtar M.A.[a], Takami T.[a] and Horio M.[b],*
[a] Dept. of Mech. Eng., Okayama University of Science, Okayama 700-0005, Japan
[b] Dept of Chem. Eng., Tokyo University of Agriculture and Technology.,
Koganei, Tokyo 184-8588, Japan

ABSTRACT

The aim of the present work is to establish a model of heat transfer between particles by using the numerical simulation that can be incorporated in the discrete element method (DEM). The contact heat transfer between particles can be regarded as a contact thermal resistance problem. In the thermal resistance model, the local characteristics, e.g. exact contact area and heat flux distribution on particle surface, are important. However, it is difficult to measure such factors in detail. Accordingly, the authors utilized a numerical simulation. The thermal resistance was modeled by placing a small solid block between the contacting areas in the simulation. The small solid thickness represents the surface roughness and the width represents the contact force. The simulated temperature profile along the center line through two particle's centers well agreed with measured one.

INTRODUCTION

In the development of fluidized bed, the Discrete Element Method (DEM) has recently been used for the heat transfer problems and also for trouble analyses. DEM is a very useful tool to analyze the various powder processes. It is possible to deal with many problem-factors in the level of particle size with DEM. For example, Rong and Horio (1) used DEM to conduct a fluidized-bed combustion simulation and obtained remarkable results. Morikawa et al. (2) used DEM to analyze the heat and flow in a fluidized bed combustor and obtained a good qualitative agreement of the heat transfer coefficient between bed and heat transfer tube. However, the equation to estimate contact heat transfer between colliding particles has not been validated sufficiently.

Accordingly, the authors measured the heat transfer between the contacting particles (3). According to the definition of DEM calculation, the heat transfer was classified into 3 groups, i.e. convection heat transfer, conduction heat transfer, and contact heat transfer. From the results, the estimated values of convection and conduction heat transfers well agreed whereas estimated contact heat transfer poorly agreed

with the measured one(3). The authors (4) then adopted the thermal resistance model to estimate the contact heat transfer between two contacting particles. The contact heat transfer calculated with the thermal resistance model showed better agreement than with the model of Rong and Horio (1). Furthermore, an interesting tendency was obtained. The measured heat transfer increased as the surface roughness increased. This would be caused by the effect of the increase in the contact area accompanied by the increase of surface roughness. These results also indicate that the effect of surface roughness on contact heat transfer is change.

In order to estimate the amount of the contact heat transfer between two contacting particles in detail, the heat and flow around particles were analyzed with numerical simulation and also with the experiments. In the present simulation, a small solid was set between the contacting particles to simulate the characteristic of thermal resistance.

By these analyses, the present work was carried out to establish a heat transfer model that can be incorporate into DEM simulation with the thermal resistance model to the contact heat transfer between two contacting particles.

THEORETICAL ANALYSIS

Numerical simulation

The problem schematic is shown in Fig. 1. The radius and height of the cylindrical area are 0.12m and 0.14m. The sphere size used in the simulation is 0.0191m and the characteristics of the sphere are same as SUS304 used in the experimental one.

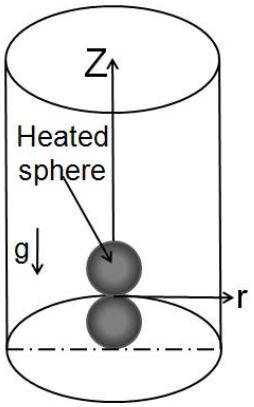

Fig. 1 Problem Schematic

For the numerical simulation, the upper particle was heated to 50, 100 and 150^{o}C. The lower particles were set at 23^{o}C as well as the room temperature. This state was set as the initial condition for simulation.

The properties of the sphere and air used in the simulation are indicated in Table 1. It is assumed that the flow and temperature are axisymmetric in the present analyses. For the numerical simulation, FLUENT 6.1.22 was utilized. The computational mesh grid system for the present simulation is shown in Fig. 2.

Table 1. Properties of sphere and air

Properties	sphere	air
ρ(kg/m^3)	7930	1.205
c_p (J/kgK)	500	718
λ(W/mK)	1,5,8,16.8	0.0257
μ(Pa·s)	-	1.512×10^{-5}

For the boundary conditions are shown as follow:

For velocity,

$$\vec{v} = 0 \quad \text{at} \quad r=r_{out} \tag{1}$$

$$v_r = 0, \frac{dv_z}{dr} = 0 \quad \text{at} \quad r=0 \tag{2}$$

$$\frac{dv_r}{dz} = \frac{dv_z}{dz} = 0 \quad \text{at } z=h,-d_p \tag{3}$$

$$\vec{v} = 0 \quad \text{on sphere surface} \tag{4}$$

For temperature,

$$T = 23°C \quad \text{at} \quad r=r_{out} \tag{5}$$

$$\frac{\partial T}{\partial r} = 0 \quad \text{at} \quad r=0 \tag{6}$$

$$T = 23°C \quad \text{at} \quad z= -d_p \tag{7}$$

$$\frac{\partial T}{\partial z} = 0 \quad \text{at} \quad z=h \tag{8}$$

Modeling of the thermal resistance

If the thermal resistance exactly is considered in a numerical simulation, the shape of roughness should be taken into account. Since the scale of surface roughness is 0.1 μm-10μm, it is almost impossible to simulate with the present method. Accordingly, thermal resistance was modeled by a small solid in the present work. A small solid was inserted between the contacting particles in the numerical simulation as shown in Fig. 3. The radius and thickness of the small solid is 2.5mm and 1mm. Analogy of the thermal conductivity and thermal resistance are shown below.

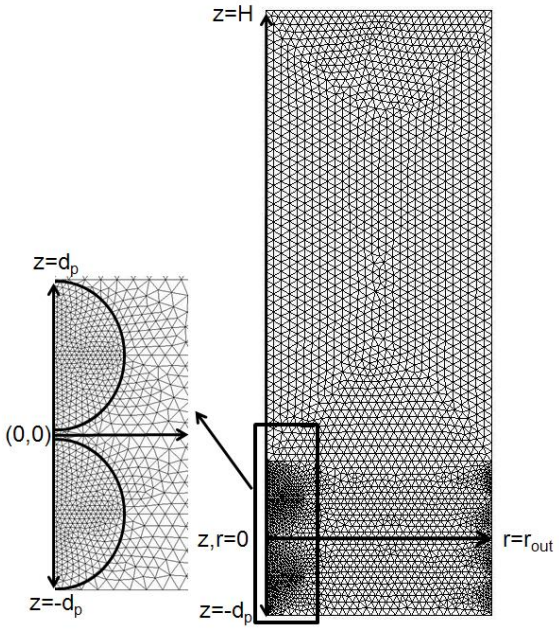

Fig. 2 Computational Mesh

$$q = h_m(\theta_h - \theta_c) \longrightarrow q = \frac{\lambda}{\delta}(\theta_h - \theta_c) \tag{9}$$

From equation (9), $1/h_m$ are equal to thermal resistance and λ/δ are the equivalent conductivity. The thermal conductivity of the small solid is changed to obtain the value equivalent to the thermal resistance.

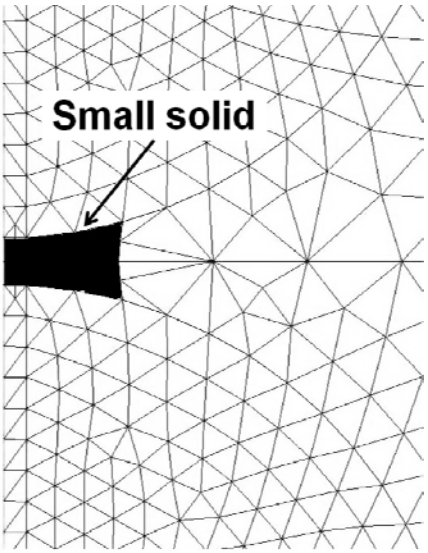

Fig. 3 Small solid size mesh at contacting region

In the experiment, the surface roughness of the stainless steel (SUS304) sphere was measured with Laser Microscope VK-9710, (KEYENCE Co., Ltd., Japan, VK-9700).

EXPERIMENT

Two stainless steel spheres (SUS304) were utilized as particles and the size of the spheres are 19.1mm. Two particles are set in horizontal array and statically in contact as shown in Fig. 4. In order to reduce disturbance, the analysis domain was surrounded by an acrylic cylindrical tube at the radius and height of 0.12m and 0.14m.

The stainless steel spheres were painted in black color to reduce the reflection for the IR measurement before heated. The temperature differences between the non-painted and painted spheres were 1-2^{o}C and it can be ignored. The upper sphere was heated to 50, 100 and 150^{o}C while the lower sphere was set to be at the same temperature of air at 23^{o}C. This state was set as the initial condition, and the two spheres were then brought into contact.

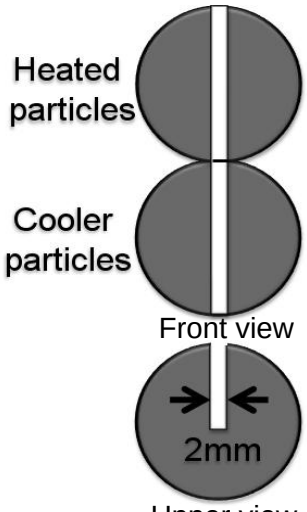

Fig. 4 Groove particles for temperature distribution

The temperature distribution along the center axis was measured with particles with a groove as shown in the Fig. 4. The temperature on the groove, i.e. th temperature on the center axis was observed with Infra-Red (IR) thermal imager (5) (NEC san-ei Instruments Ltd., Japan, TH9100 PMV). The temperature distribution then was calculated using the thermal imager software (TH91-703). On the other hand, the temperature distribution of gas phase was observed with a Mach-Zehnder interferometer (Mizojiri Optical Co., Ltd., Japan).

The flow around the two contacting spheres was measured with a Particle Imaging Velocimetry (PIV) system (TSI Inc, USA). The PIV system consists mainly of a double-pulse Nd: YAG Laser (BM industries, SERIE 5000: wave length: 532 nm, 10 mJ-3J/Pulse) and a CCD camera (TSI Inc, 7PIVCAM 10-30, Model 630046), which is capable of recording at 30 fps with a resolution 1,000×1,016pixels.

RESULTS AND DISCUSSION

Flow visualized around the contacting spheres

In order to validate the numerical simulation, the simulated flow pattern and temperature distribution of gas between the contacting spheres were compared with the experimental one (3). Fig. 5 shows the flow pattern around the contacting spheres. The figure was taken at the time t=1s. The flow caused by natural convection can be observed around the contacting particles in both the experiment (3) and simulation. The stagnant region near the contacting point can be seen. The area of this stagnant region is almost the same as the experimental one (3).

On the other hand, Fig. 6 shows the isotherms visualized from the simulation around the contacting particles. The simulated temperature distribution well agreed with the experimental one (3).

From these results, the validity of the numerical simulation model almost was confirmed.

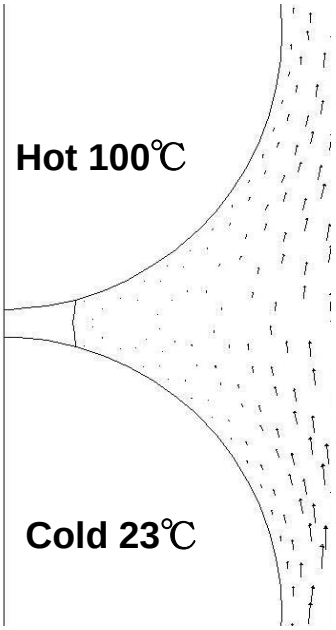

Fig. 5 Velocity vectors of gas flow

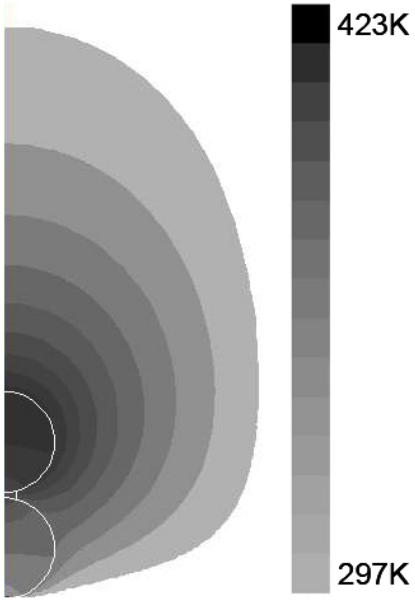

Fig. 6 Isotherms at the stagnant region

Temperature distribution along center axis

Fig. 7 shows the temperature distribution along the center axis for (a) experiment, (b) simulation at λ=16.8 W/mK, (c) simulation at λ=1 W/mK and (d) simulation at λ=0.5 W/mK which goes through the two spheres center, from t=0s until t=300s for the initial temperature at 100^{o}C. For the simulation at Fig. 7(b), the thermal conductivity of 16.8W/mK corresponds to no thermal resistance, i.e. perfect contact. The heat from the upper sphere was transferred to the lower sphere and the both of the sphere

temperature are almost equal at the time 300s. By comparing with experimental data in Fig. 7(a), the thermal conductivities should be lower than 16.8W/mK. From the simulated results, Fig. 7(c) with the thermal conductivity λ=1W/mK gives the best agreement with the experiment in Fig. 7(a).

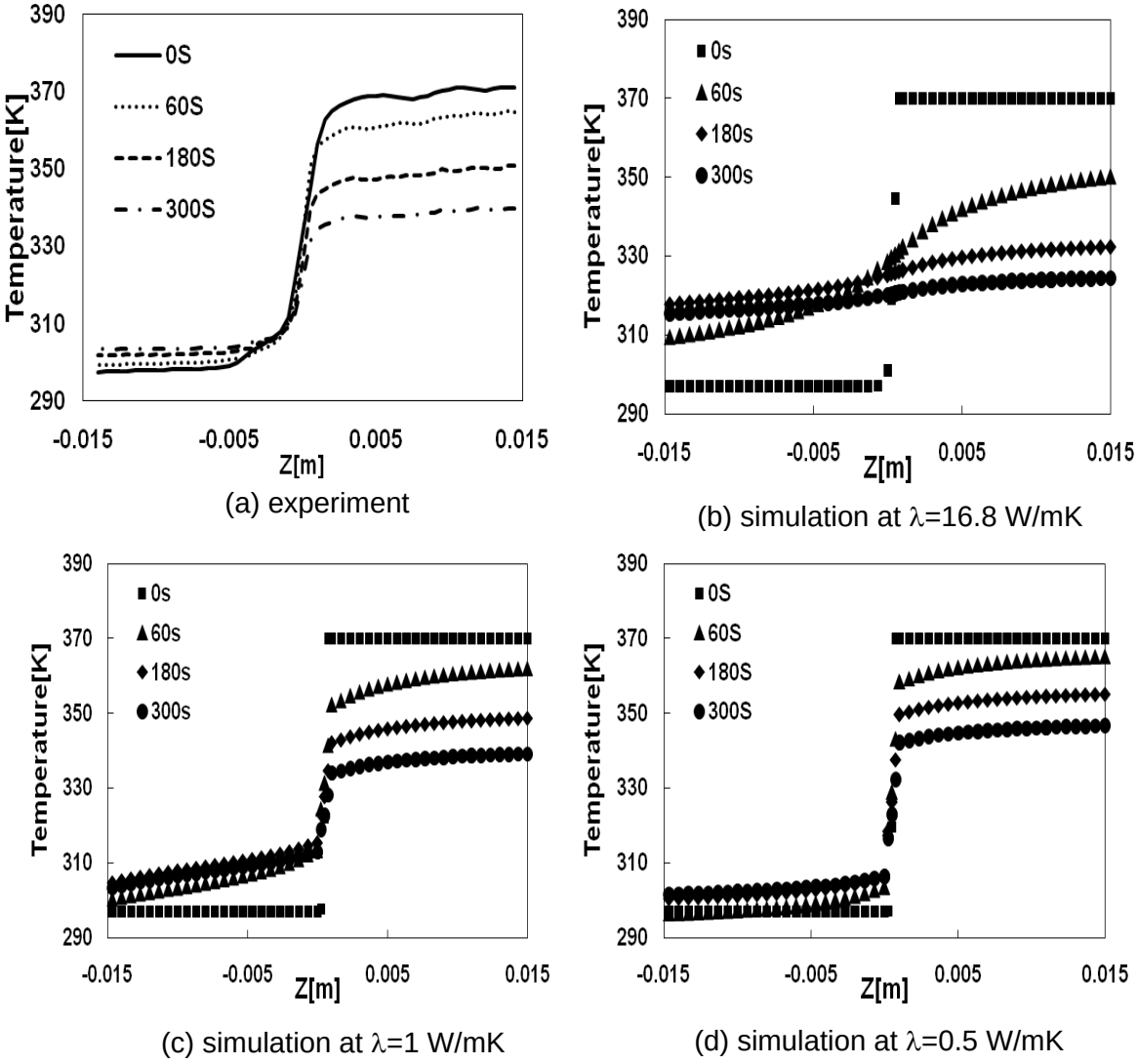

(a) experiment

(b) simulation at λ=16.8 W/mK

(c) simulation at λ=1 W/mK

(d) simulation at λ=0.5 W/mK

Fig. 7 Temperature distribution along center axis (a) experiment, (b) simulation (λ=16.8 W/mK), (c) simulation (λ=1 W/mK) and (d) simulation (λ=0.5 W/mK)

Fig. 8 shows the temperature distribution along the center axis for the initial temperature at 150^{o}C. Fig. 8(c) as the thermal conductivity is λ=1W/mK gives the best agreement as the previous result. Fig. 9 shows temperature change over time at the sphere's center with various thermal conductivities. The thermal conductivities in the simulation are 0.5, 1, 3, 8, and 16.8W/mK. Fig. 9(a) shows the simulated results started at the temperature of 100^{o}C and Fig. 9(b) shows those started at the temperature of 150^{o}C.

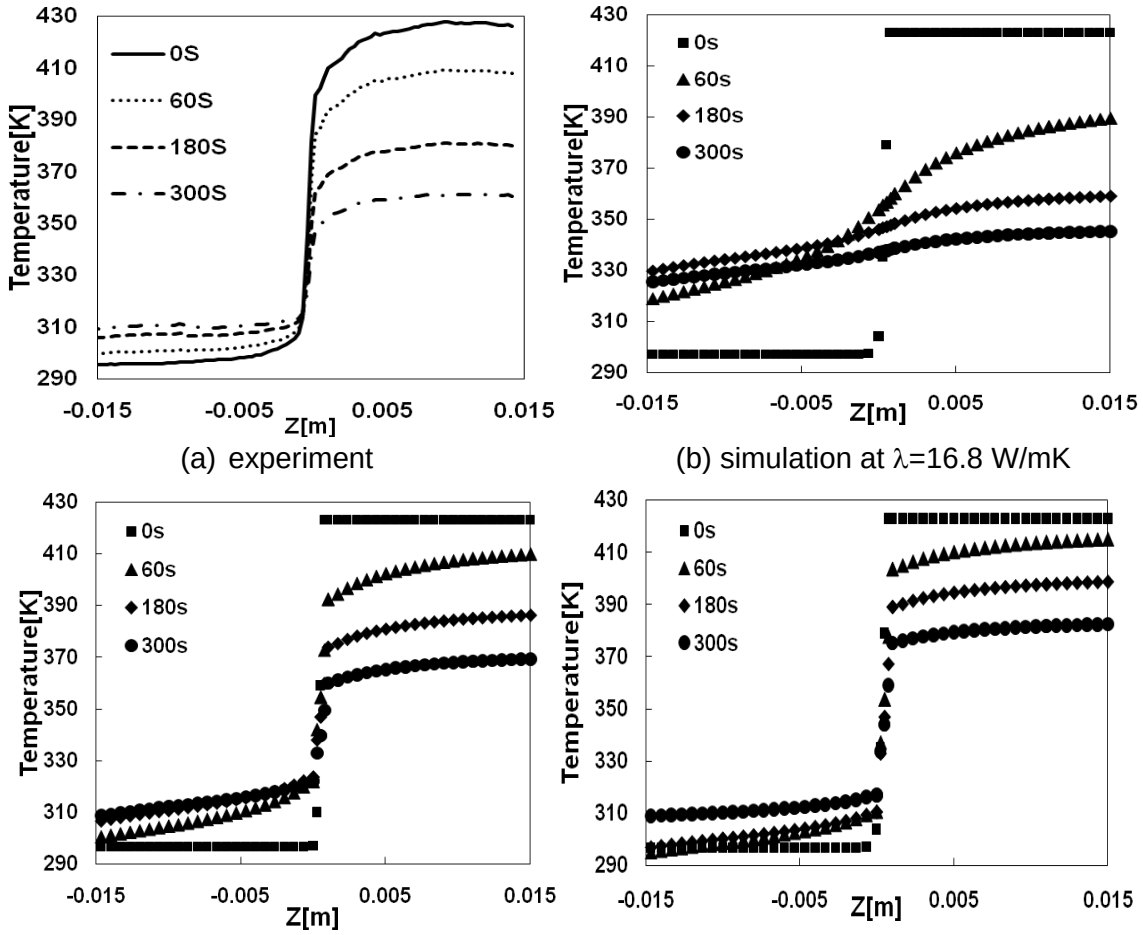

(a) experiment

(b) simulation at λ=16.8 W/mK

(c) simulation at λ=1 W/mK

(d) simulation at λ=0.5 W/mK

Fig. 8 Temperature distribution along center axis (a) experiment, (b) simulation (λ=16.8 W/mK), (c) simulation (λ=1 W/mK) and (d) simulation (λ=0.5 W/mK)

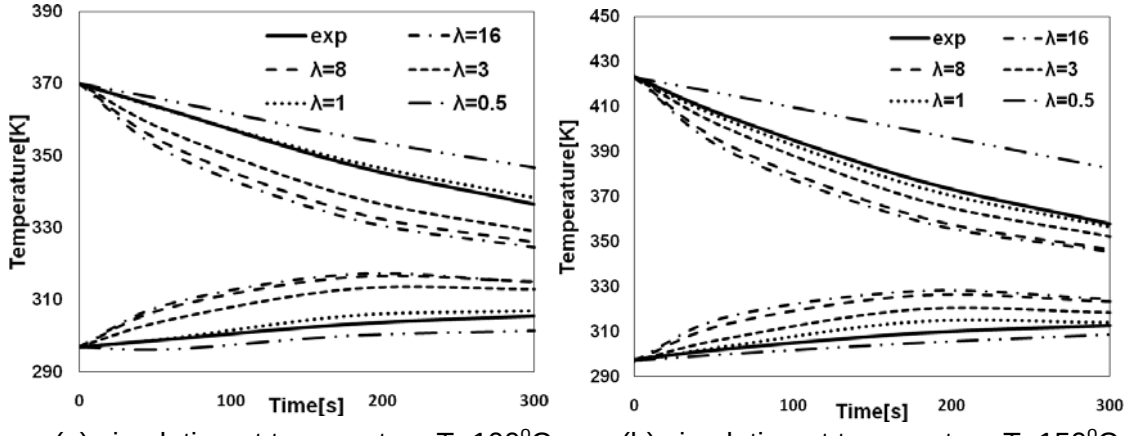

(a) simulation at temperature T=100°C

(b) simulation at temperature T=150°C

Fig. 9 Validation in temperature at spheres center

From Fig. 9, when the thermal conductivity is at 16.8 W/mK there is no thermal resistance but the experiment result shows differently. The thermal conductivity of 1 W/mK gives the best agreement with the experimental one in both cases.

CONCLUSIONS

A small solid was used to simulate thermal resistance between two contacting particles. As a result, temperature distribution that was caused by the thermal resistance were able to be reproduced. From Fig.9, it can be assume that the heat transfer decreased as the thermal conductivities of the small solid decreased. The temperature distribution simulated with the thermal conductivities of 1W/mK (SUS304:16.8W/mK) well agreed with the experimental one near the contact point.

From the present result, it was confirmed that the present model for thermal resistance is useful. When surface roughness and contact force are changes from the experiments, the witdh, thickness and conductivity of the small solid between particles in the present model should be changed. Such effect should be examined in more detail.

NOTATION

c_p	specific heat of particles(J/kgK)	Greek letters	
v	*velocity(m/s)*		
d_p	*particle diameter(mm)*	λ	Thermal conductivity(W/mK)
T	*temperature(^oC)*	μ	Viscosity coefficient(kg/ms)
g	*gravitational acceleration (m/s^2)*	ρ	Density(kg/m^3)
t	time(s)		

REFERENCES

1 Rong, D. and Horio, M., 2nd International Conference on CFD in the Minerals and Process Industries, 65-70 (1999).

2 Morikawa, H., Rong, D., and Horio, M., DEM simulation of bubbling Fluidized Bed including Char Combustion and Cooling by Immersed tubes (in japanese), 182-188 (2000)

3 Kuwagi, K., Hirano, H. and Takami, T., Experimental and Numerical Study on Heat Transfer Between Two Spheres, JP Journal of Heat and Mass Transfer, Vol. 1 (1), 49-61 (2007).

4 Kuwagi, K., Mokhtar, B, M, Arif., Takami, T., Analysis of Heat Transfer between Two Particles for DEM simulations, Fluidization XII, paper 28 (2007)

5 Sakurai, T., Minami, T., and Kawaguchi, T., DEM-CFD Simulation and Thermography Measurement of Fluidized Bed with Heat Transfer (Fluid Engineering) (in Japanese), The Japan Society of Mechanical Engineering, 1041-1048 (2009)